

## **BEND STIFFNER LINEAR VISCOELASTIC RESPONSE SUBJECTED TO HARMONIC LOADING**

**Murilo Augusto Vaz, murilo@peno.coppe.ufrj.br**

**Marcelo Caire, caire@peno.coppe.ufrj.br**

Ocean Engineering Department, Federal University of Rio de Janeiro, Rio de Janeiro, Brazil

**Aynor Ariza Gómez, ajariza@peno.coppe.ufrj.br**

**Luiz Felipe Azevedo Farias, lufefarias@peno.coppe.ufrj.br**

***Abstract.** Bend stiffeners are components for flexible risers and umbilical cables employed to ensure a safe transition at the riser-vessel interface, limiting bending stresses and curvature to acceptable levels. The analysis and design of bend stiffeners usually consider the riser/stiffener system as a unique beam subjected to a static extreme tension-angle loading condition obtained from global analysis and applied near the tip of the stiffener. The polyurethane used for bend stiffener manufacture is usually considered linear or non-linear elastic. In this paper the stiffener body is represented by a linear viscoelastic material subjected to a harmonic tension-angle tip loading and the effect of loading frequency and phase lag evaluated. A set of creep experiments using stiffener polyurethane samples is carried out to obtain the time dependent material constitutive behavior. The set of four non-linear ordinary differential equations is derived from geometrical compatibility, equilibrium of forces and moments and constitutive equations. The numerical solution is obtained using the fourth order Runge-Kutta method. A finite element analysis with the same hypotheses is carried out to compare and validate the analytical model. A case study is presented considering several loading conditions where the frequency and phase-lag parameters vary while the amplitude is kept constant.*

**Keywords:** bend stiffener, viscoelastic, harmonic loading

### **1. INTRODUCTION**

The flexible pipe top connection with the platform is a critical point regarding the maximum allowed curvature and fatigue life because this region is susceptible to the highest stresses due to static and dynamics loads. The stiffness transition between the flexible pipe and the rigid platform is achieved using a conical shape structure made of polyurethane called bend stiffener. This is an effective way to prevent the riser failure from overbending and from accumulation of fatigue damage. Besides, the stiffener must be designed to ensure its own fatigue lifetime. The conventional bend stiffener design usually account for extreme loading condition obtained from global motion analysis to ensure the flexible riser does not bend below the allowable minimum bending radius (MBR). The MBR is normally determined from a maximum allowed bending strain in the flexible pipe outer sheath (e.g. 7%) and provides a clear limit state in designing the bend stiffener. A global motion analysis of a flexible riser is the first stage in the design of a stiffener and consider a pinned boundary condition on the platform. The main output of global analysis for the stiffener design is the tension and angle distribution at the pinned end connection.

The analysis and design of bend stiffeners represented by an equivalent beam were previously presented. Vaz *et al* (2007) introduced the polyurethane material non-linearity and extended Boef & Out (1990) model. Caire *et al* (2005) presented a model considering the polyurethane with viscoelastic response subjected to a static load. The previous authors considered in all cases a static loading condition applied to the system. A question that arises when dealing with a time dependent material, such as the polyurethane, is the effect of the actual loading conditions applied to the flexible pipe/stiffener system during operation.

In this work the effect of varying the frequency and phase lag parameters when considering a harmonic loading applied to the system with a linear viscoelastic polyurethane is evaluated. Experimental tests are carried out to obtain the polyurethane viscoelastic response using samples cut from an existent bend stiffener. The mathematical formulation and a method of solution for the riser/bend stiffener is presented. The numerical solution obtained using an iterative Runge-Kutta method is compared to the results obtained using the commercial finite element software Abaqus v6.8. A case study is presented for several loading conditions and the results discussed.

### **2. CREEP TEST**

The creep test measure the dimensional changes that occur along time under a static load. Usually many stress levels are applied in a selected loading configuration (tension or compression) at constant temperature and the deformation is measured as a function of time to characterize a polyurethane behavior. In the analysis it is assumed that the load is applied instantaneously and remains constant after application. As it is impossible to achieve because of the dynamics of the system, the load is applied gradually over a short time period to avoid vibration and using different rates to evaluate its effect.

A viscoelastic material may be considered linear if the stress level applied is proportional to strain at a given time and the superposition principle holds. Although most of the polyurethane materials present nonlinear behavior even for

small strain, the linear behavior is assumed here, in order to simplify the mathematical formulation and consequently, only one stress level is applied in the sample. The set of experimental tests are carried out at room temperature using samples cut from an actual bend stiffener where the standard ASTM D 2990 is adopted. Two strain rates (50, 100 mm/min) are applied using a Instron servo-hydraulic testing machine to reach a specified stress level (2.6 MPa). Three samples for each strain rate are used in order to obtain a mean representative curve. The duration of each test is approximately 900 sec. The strain is measured by use of an extensometer and the engineering stress using the applied force and undeformed area. The following one dimensional constitutive equation may be employed according to Wineman & Rajagopal (2000) in order to characterize the material behavior,

$$\varepsilon(s, \tau) = \int_0^t J(s, \tau) \cdot \frac{\partial \sigma(t - \tau)}{\partial (t - \tau)} d\tau \quad (1)$$

The creep curve  $J(t)$  is adjusted using a third order Prony series as follows,

$$J(t) = J_0 + J_1 \cdot e^{-t/\tau_{c1}} + J_2 \cdot e^{-t/\tau_{c2}} + J_3 \cdot e^{-t/\tau_{c3}} \quad (2)$$

The hypothesis of a constant static load may be employed if only the long term behavior is sought, which is not the case herein. It can be seen in Fig. 1 that the stress starts to stabilize after approximately 10s and consequently the whole strain and stress history is used to adjust the creep curve using Eq. (1) and (2). The obtained creep coefficients are,

Table 1 - Creep coefficients

$J_0$ (MPa <sup>-1</sup> )	$J_1$ (MPa <sup>-1</sup> )	$J_2$ (MPa <sup>-1</sup> )	$J_3$ (MPa <sup>-1</sup> )	$\tau_{c1}$ (s)	$\tau_{c2}$ (s)	$\tau_{c3}$ (s)
0.02915	-0.010843	-0.0028107	-0.003782	1.448	32.477	332.346

and the adjusted curve is shown in Fig. 2. According to Wineman & Rajagopal (2000) once the creep curve is obtained, the relaxation curve  $G(t)$  may be numerically calculated using the following relation,

$$1 = J(t) \cdot G(0) + \int_0^t J(s) \cdot G'(t - s) \cdot ds \quad (3)$$

Using Eq. (3), the relaxation coefficients are found as,

Table 2 - Relaxation coefficients

$G_0$ (MPa)	$G_1$ (MPa)	$G_2$ (MPa)	$G_3$ (MPa)	$\tau_{R1}$ (s)	$\tau_{R2}$ (s)	$\tau_{R3}$ (s)
34.305317	41.304121	4.802776	4.952019	0.75	28.908	289.826

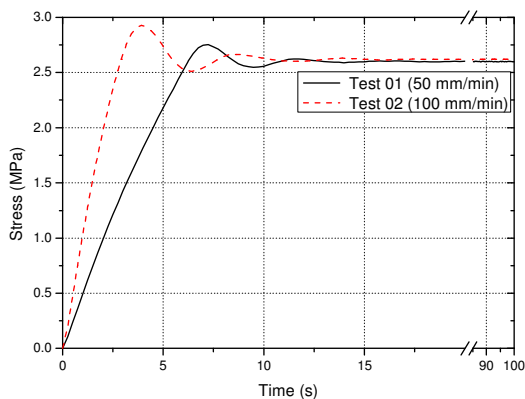


Figure 1 – Stress x Time

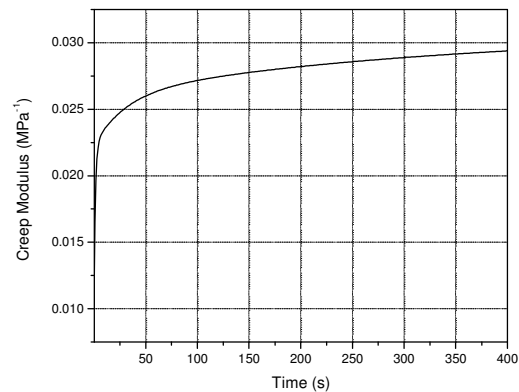


Figure 2 - Creep function x Time

If the initial time  $t = 0$  is considered, a representative stiffer Young modulus may be found using the relaxation function as  $G(0) = 85.3 \text{ MPa}$ .

### 3. ANALYTICAL FORMULATION

The current practice for the design of bend stiffeners is to first consider the system as a slender beam model subjected to the extreme load parameters combination  $(F, \theta_L)$  obtained from the global analysis without the stiffener in an iterative procedure until a final design meet the system requirements. If local information is required, such as the stress distribution in the insert region, a three-dimensional finite element analysis may be employed. In the present study the beam model approach is developed with the following assumptions: a) the cross section undergoes large displacements; b) the axial extensibility is neglected; c) the gap between the structures is disregarded; d) the flexible pipe is considered with a constant bending stiffness along length; e) the polyurethane is represented by a linear viscoelastic constitutive model and f) dynamic response due to system mass is disregarded.

The set of four first order non-linear ordinary integro-differential-partial equations are obtained considering the geometrical compatibility, equilibrium of forces and moments and linear viscoelastic constitutive relations. Figure 3 shows a schematic figure of the flexible pipe/bend stiffener system and Fig. 4 an infinitesimal element.

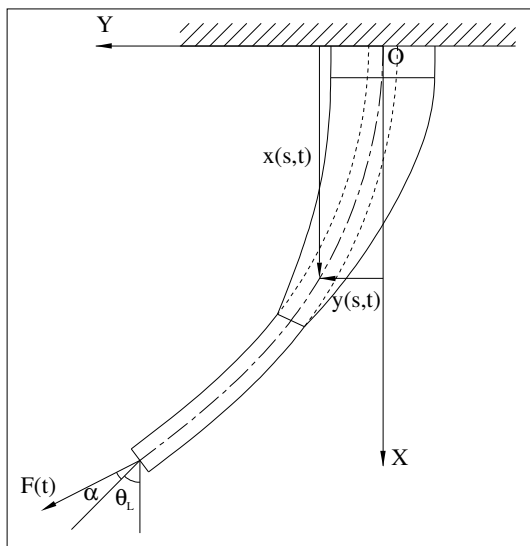


Figure 3 – Schematic of the Riser/Bend stiffener

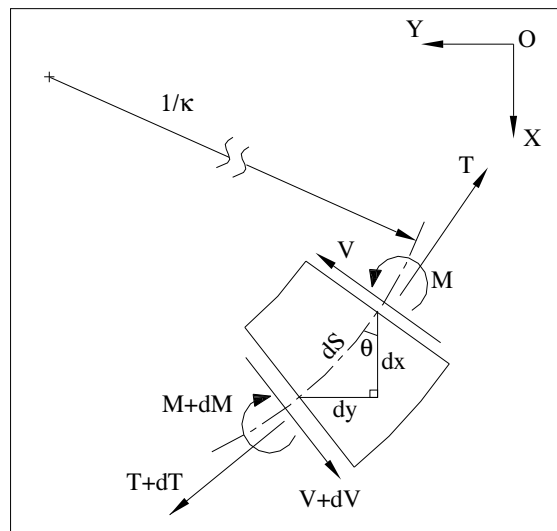


Figure 4 – Infinitesimal Element

#### 3.1. Geometrical relations

Applying trigonometrical relations to the infinitesimal element shown in Fig. 4, the following equations are found,

$$\frac{\partial x(s,t)}{\partial s} = \cos(\theta(s,t)) \quad (4)$$

$$\frac{\partial y(s,t)}{\partial s} = \sin(\theta(s,t)) \quad (5)$$

In addition, the curvature may be defined by,

$$\frac{\partial \theta(s,t)}{\partial s} = k(s,t) \quad (6)$$

where  $s$  is the rod arc-length measured from the fixed end,  $(x(s,t), y(s,t))$  are the Cartesian coordinates of the deflected rod that varies with time,  $\theta(s,t)$  is the slope with respect to the  $x$ -axis of any point along the arc length and  $k(s,t)$  is the curvature.

### 3.2. Equilibrium of forces and moments

Considering static equilibrium, the force and moment reactions may be calculated in the origin of the Cartesian axis from the loading conditions  $(F(t), \alpha, \theta_L(t))$ . The tension  $T(s, t)$ , shear force  $V(s, t)$  and bending moment  $M(s, t)$  can be easily determined as follows

$$\begin{cases} V(s, t) = -F(t) \cdot \sin(\theta_L(t) + \alpha - \theta(s, t)) \\ T(s, t) = F(t) \cdot \cos(\theta_L(t) + \alpha - \theta(s, t)) \\ M(s, t) = F(t) \cdot \sin(\theta_L(t) + \alpha) \int_s^L \cos \theta(s, t) \cdot ds \\ \quad - F(t) \cdot \cos(\theta_L(t) + \alpha) \int_s^L \sin \theta(s, t) \cdot ds \end{cases} \quad (7)$$

Differentiating the bending moment with respect to  $s$ ,

$$\frac{\partial M(s, t)}{\partial s} = -F(t) \cdot \sin(\theta_L(t) + \alpha - \theta(s, t)) \quad (8)$$

Supposing the linearity of viscoelastic response (i.e., the material behavior is independent on the stress or strain levels), homogeneous and isotropic material and considering pure bending where each material element is in a uniaxial stress state, the following constitutive equation may be employed according to Wineman & Rajagopal (2000) to the bend stiffener polyurethane,

$$\begin{aligned} \sigma_{BS}(t) &= \varepsilon(s, t) \cdot G(0) + \int_0^t \varepsilon(s, \tau) \cdot \frac{\partial G(t - \tau)}{\partial (t - \tau)} \cdot d\tau \\ &= \int_0^t \varepsilon(t - \tau) \cdot dG(\tau) \end{aligned} \quad (9)$$

where  $t$  is the current time,  $\tau$  is a representative previous time,  $\sigma_{BS}(s, t)$  is the normal stress,  $\varepsilon(s, t)$  is the axial strain and  $G(t)$  is the relaxation function as previously described. The flexible pipe stress x strain relation may be approximated by a linear relation that leads to a constant bending stiffness along length,  $EI_{PIPE}$ . Assuming that plane sections remain plane after bending implies that the axial strain at a given time  $t$  varies linearly with the distance from the neutral axis  $y$  and is described by,

$$\varepsilon(y, s, t) = y \cdot k(s, t) \quad (10)$$

The equilibrium of bending moments for the cross-section area of the system yields,

$$M(s, t) = \int_{A_{PIPE}} \sigma_{PIPE} \cdot y \cdot dA + \int_{A_{BS}} \sigma_{BS} \cdot y \cdot dA \quad (11)$$

where the subscript BS indicates the bend stiffener and PIPE refers to the flexible pipe. Using Eq. (9), (10) e (11), we find the bending moment x curvature relation for the system,

$$M(s, t) = EI_{PIPE} \cdot k(s, t) + I_{BS}(s) \cdot \int_0^t k(s, t - \tau) \cdot dG(\tau) \quad (12)$$

and  $I_{BS}(s) = \int_{A_{BS}} y^2 dA$ , is the second moment of area for the bend stiffener. Differentiating equation (12) with respect to position, introducing Eq. (8), expanding the Riemann-Stieltjes integral and algebraically manipulating, the following governing equation is found,

$$\begin{aligned} \frac{\partial k(s,t)}{\partial s} = & -\frac{1}{EI_{PIPE} + G(0)I_{BS}(s)} \frac{dI_{BS}(s)}{ds} \left( G(0)k(s,t) + \int_0^t k(s,\tau) \frac{\partial G(t-\tau)}{\partial(t-\tau)} d\tau \right) \\ & - \frac{1}{EI_{PIPE} + G(0)I_{BS}(s)} I_{BS}(s) \int_0^t \frac{\partial k(s,\tau)}{\partial s} \frac{\partial G(t-\tau)}{\partial(t-\tau)} d\tau \\ & - \frac{1}{EI_{PIPE} + G(0)I_{BS}(s)} \cdot F(t) \cdot \sin(\theta_L(t) + \alpha - \theta(s,t)) \end{aligned} \quad (13)$$

### 3.3. Boundary conditions

The geometrical relations (4) to (6) and Eq. (13) form the system of four non-linear ordinary differential equations that represent the boundary value problem. The following four boundary conditions are specified to solve the problem,

$$\begin{cases} x(0,t) = 0 \\ y(0,t) = 0 \\ \theta(0,t) = 0 \\ \theta(L,t) = \theta_L(t) \end{cases} \quad (14)$$

### 4. NUMERICAL SOLUTION

The resultant system of four non-linear integro-differential-partial equations is solved for each time  $t$  using a one-parameter shooting method which converts the boundary value problem into an equivalent initial value problem. The mathematical package Mathcad has been employed in the algorithm implementation. Fixed end curvatures are guessed for the current time and then the system of equations is integrated using a fourth-order Runge-Kutta method with a trial-and-error approach. The Simpson's one-third rule is employed to the hereditary integral. This method is used to incrementally solve the system from the initial time up to a final specified time. Each solution obtained from a previous time is required to solve the problem in the current time as can be observed in the hereditary integral of equation (13).

### 5. FINITE ELEMENT MODEL

Using the same assumptions as per in the analytical procedure, a finite element analysis using Abaqus v6.8 is developed in order to compare and validate the results. The analysis is divided into a static and a quasi-static step. The model similarity is achieved using the following: a) two dimensional Euler-Bernoulli beam element B23 is used to generate the beam mesh; b) the Nlgeom parameter is included in the \*Step command to indicate that geometric nonlinearity should be accounted for during the step as the problem undergoes large displacements; c) the option \*Visco is used to obtain a transient static response in an analysis with viscoelastic material behavior; d) the command \*Tie ensures that the stiffener and pipe nodes have the same degree of freedom, i.e., there is no relative displacement nor gap. A Fortran subroutine is developed to generate the nodes, elements and section properties along the system length and to get the results from the high number of analysis performed.

### 6. CASE STUDY

The example considered in the case study is a 3.2 m long flexible riser segment with an internal diameter of 10.2 cm. The riser external diameter and bending stiffness are respectively: 18 cm and 10 kN.m<sup>2</sup>. The bend stiffener and system geometry are shown in Fig. 5

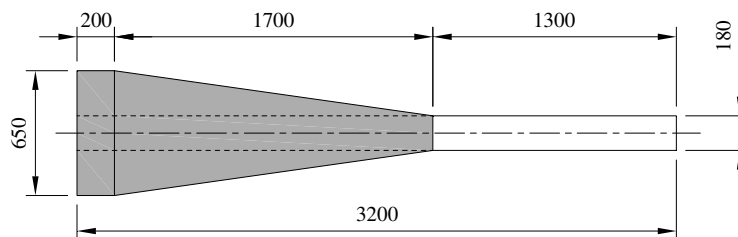


Figure 5 – System Geometry

A harmonic angle-force loading condition is applied as follows,

$$\begin{cases} F(t) = \bar{F} + \Delta F \cdot \sin[(2\pi f)t] \\ \theta_L(t) = \bar{\theta}_L + \Delta\theta_L \cdot \sin[(2\pi f)t - \delta] \end{cases} \quad (15)$$

where  $\bar{F}$  and  $\bar{\theta}_L$  are the mean top tension and end rotation respectively,  $\Delta F$  and  $\Delta\theta_L$  are the amplitudes,  $f$  is the loading frequency and  $\delta$  is the phase lag. In order to simulate the static and dynamic loads applied to the system and evaluate the effect of different loading frequencies and phases, the following coefficients are used in the case study,

Table 3 - Load coefficients

$\bar{F}$	62.5, 500 kN
$\bar{\theta}_L$	45°
$\Delta F, \Delta\theta_L$	0.2
$f$	0.01 - 1 Hz
$\delta$	0,30,60,90°

The numerical solution obtained using an iterative Runge-Kutta method and the finite element analysis performed using software Abaqus v6.8 demonstrated total agreement, hence validating the method adopted. The results for maximum curvature versus frequency for all phase lags applied are presented in Fig. 6 and 8. Figures 7 and 9 show the maximum curvature variation,  $\Delta k$ , in one cycle versus frequency as  $t \rightarrow \infty$ . It's worth noting that the curvature distribution is non-uniform along length and the maximum curvature does not necessarily occurs at the encastre. As the mean load decreases from  $\bar{F} = 500 \text{ kN}$  to  $62.5 \text{ kN}$  the location of the maximum curvature shifts from the encastre towards the free end. As the riser is subjected to several operational loading conditions, the critical section in terms of fatigue life should be carefully assessed.

$$\bar{F} = 62.5 \text{ kN}$$

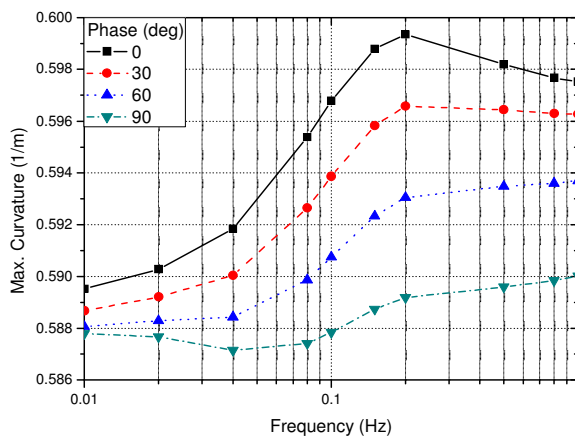


Fig. 6 - Max. Curvature x Frequency

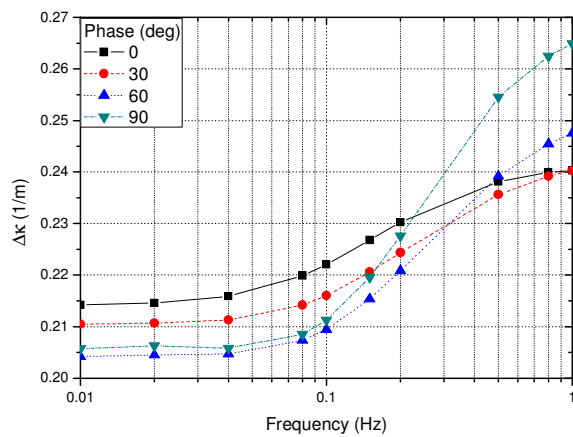


Fig. 7 - Curvature Variation x Frequency

$$\bar{F} = 500 \text{ kN}$$

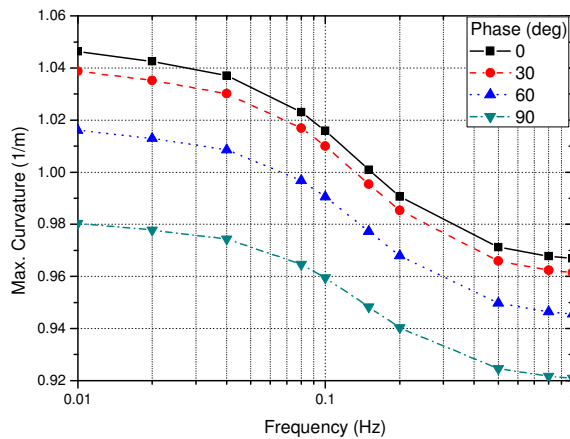


Fig. 8 - Max. Curvature x Frequency

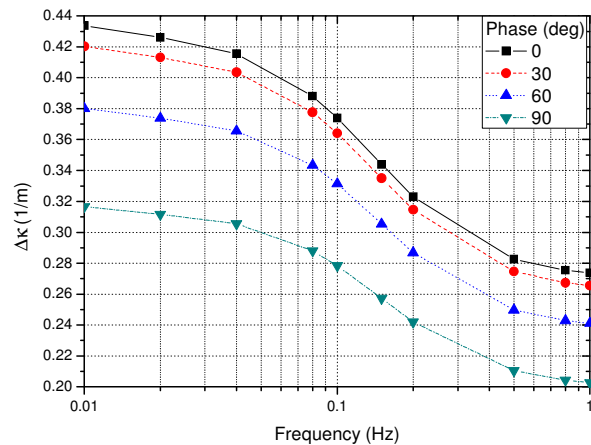


Fig. 9 - Curvature Variation x Frequency

It can be observed from the results that for the first case ( $\bar{F} = 62.5 \text{ kN}$ ), as the frequency of the applied load increases, there is a general tendency to increase the maximum curvature. For the second case, where a higher load is applied ( $\bar{F} = 500 \text{ kN}$ ), the opposite occurs and the maximum curvature decreases as the frequency increases. For both cases, the lowest the phase lag, the highest the curvature value. From Fig. 6 and 8, the highest increase that occur for the maximum curvature value along length for  $62.5 \text{ kN}$  is approximately 2% while for  $500 \text{ kN}$ , is 12%.

As can be seen in Fig. 7 and 9, the cyclical curvature component  $\Delta k$  may be highly affected by the frequency and phase parameters. Considering, for example, the combination  $\delta = 0$  and  $f = 0.01 \text{ Hz}$  one found  $\Delta k = 0.434 \text{ (1/m)}$  when applying  $\bar{F} = 500 \text{ kN}$ . If the phase increase to  $\delta = 90^\circ$  and the frequency to  $f = 1 \text{ Hz}$ , we obtain  $\Delta k = 0.203 \text{ (1/m)}$ , that means a decrease of approximately 113%. Conversely, for the mean load  $\bar{F} = 62.5 \text{ kN}$  there is an increase of approximately 30%. The results presented demonstrate that a correct viscoelastic material characterization and load determination from the global analysis are important aspects to be considered for the design and analysis of bend stiffeners, especially for fatigue life, as the harmonic loading may highly affect the cyclical curvature component  $\Delta k$ .

## 7. CONCLUSIONS

This paper presents the mathematical formulation and a numerical solution method for the large deflection analysis of the flexible pipe/bend stiffener system used in the offshore industry. The polyurethane stiffener body is represented by a linear viscoelastic model. Creep tests are carried out with the polyurethane cut from an actual bend stiffener in order to characterize its response and the curves were adjusted using the Prony series. The mathematical formulation representing the system as a beam model is presented and an iterative Runge-Kutta method employed to obtain the solution. The numerical solution is validated through a finite element model using software Abaqus v6.8. The results presented in the case study show the importance of considering the effect of loading frequency applied to the system with a viscoelastic bend stiffener, especially for fatigue assessment.

## 8. ACKNOWLEDGEMENTS

The authors would like to thank the support of National Council for Scientific and Technological Development (CNPq), National Agency of Petroleum (ANP) and (CAPES) for this work.

## 9. REFERENCES

- Boef, W.J.C. and Out, J.M.M., 1990, "Analysis of a flexible riser top connection with bend restrictor", Offshore Technology Conference, OTC 6436, Houston
- Caire, M., Vaz, M. A. and lemos, C. A. D., 2005, "Viscoelastic Analysis of Bend Stiffeners", Offshore Mechanics and Arctic Engineering, OMAE 67321, Halkidiki.

- Smith, R., 2008, "Bending Stiffeners for Extreme and Fatigue Loading of Unbonded flexible Risers", Offshore Mechanics and Arctic Engineering,, OMAE 57464, Portugal.
- Vaz, M. A., Lemos, C.A.D. and Caire, M., 2007, "A Nonlinear Analysis Formulation for Bend Stiffeners", Journal of Ship Research, vol 51, No 3
- Wineman, A., Rajagopal, K. R., 2000, "Mechanical response of Polymers-An Introduction", Cambridge University Press.

#### **10. RESPONSIBILITY NOTICE**

The authors are the only responsible for the printed material included in this paper.